Project OSCAR: A Spacecraft Concept for In-Space Servicing of Large Satellites

Yaman Saran, Dawn Forrest, Elise Gage, Allie Croley, Sean Waddell, Zach Smith, Matthew Bahnsen, Emily Slater, Alex Filip, Angela Dojcak, Alex Barnes, March Tantisuwanna, Ryan Cruz* and Dr. Kevin A. Shinpaugh†
Kevin T. Crofton Department of Aerospace and Ocean Engineering, Virginia Tech, 1600 Innovation Drive, Blacksburg, VA 24061

OSCAR (Orbital Servicing Capture And Repair) is a modular servicing system designed to replace damaged and deprecated components for high-value client satellites. The system consists of a propulsion module and a payload module that unite in orbit after launching ride-sharing payloads to significantly reduce launch costs. The propulsion module (Asterix), once unified with the payload module (Obelix), delivers it to a series of high-value clients to perform operations such as removing and replacing old batteries to extend mission life and replace damaged components to restore functionality to the satellite. This is accomplished using four robotic manipulators equipped with modular, reconfigurable end-effectors tailored to the specific task requirements. Additionally, OSCAR features high fidelity ranged sensing and imaging equipment to offer inspection services to the main client and other nearby high-value satellites for a lower cost than component replacement.

I. Introduction

Project OSCAR is a modular and maintainable spacecraft, capable of autonomously servicing multiple client satellites to provide critical servicing functions, fulfilling the problem statement outlined in the COSMIC Capstone Challenge [1]. Its primary mission includes replacing the batteries and transmitter of NOAA-18, as well as conducting inspection operations for Landsat-8 and Landsat-9.

OSCAR's modular architecture enables compatibility with standard launch vehicle parameters. It is specifically designed for deployment through the SpaceX Rideshare Program, with the spacecraft divided into two units that launch separately and autonomously dock and unify once in orbit. The design also emphasizes ease of integration by leveraging proven servicing techniques, such as docking via the client satellite's engine nozzle, similar to Northrop Grumman's Mission Extension Vehicle-1 (MEV-1). Additionally, OSCAR incorporates a high proportion of commercial off-the-shelf (COTS) components, including its guidance, navigation, and control (GNC) systems, robotic arm, and some servicing tools.

Maintainability is a core feature of OSCAR's design, enabling multi-mission capability and reuse across a range of clients. Beyond its initial targets, including NOAA-18, Landsat-8, and Landsat-9, the system is adaptable to support future servicing opportunities. Its robotic systems are specifically designed to perform on-orbit replacement of key components.

OSCAR operates autonomously, minimizing the need for continuous human intervention. It is equipped with onboard software and sensing systems capable of identifying, diagnosing, and executing servicing tasks. For instance, a Quadclops inspection camera enables a detailed assessment of client satellites, after which OSCAR can carry out repairs using its robotic arm and onboard toolset.

OSCAR will fulfill key goals of the COSMIC Capstone Challenge, such as autonomous payload swapping on persistent platforms, on-orbit upgrading or replacement of spacecraft systems and components, and satellite inspection for failure assessment, as shown in the concept of operations shown in Figure 1. This concept outlines the full lifecycle of OSCAR, including launch and deployment, on-orbit assembly of its modular units, docking and repair operations for NOAA-18, inspection missions for Landsat-8 and Landsat-9, and end-of-life procedures.

*Undergraduate Students, Kevin T. Crofton Department of Aerospace and Ocean Engineering, Virginia Tech.
†Collegiate Professor and Faculty Advisor, Kevin T. Crofton Department of Aerospace and Ocean Engineering, Virginia Tech. Associate Fellow AIAA.

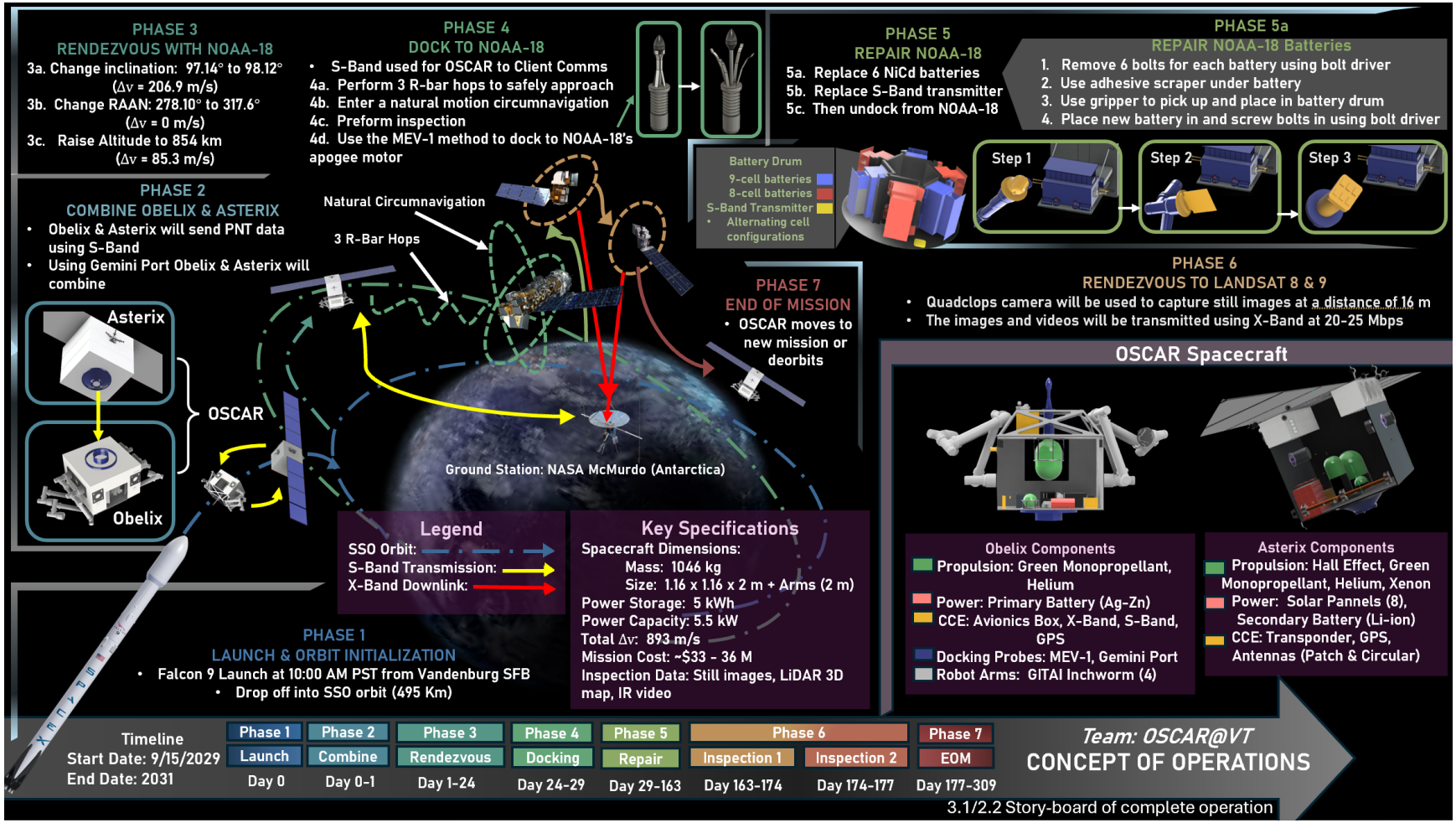

Fig. 1 OSCAR Concept of Operations. OSCAR will launch on a Falcon 9 on September 15th, 2029. The mission follows seven phases. Phase one includes the launch and orbit initialization. Phase two is where OSCAR's two modules, Asterix and Obelix, will combine into one satellite using the Gemini-style port shown. During phase three, OSCAR will rendezvous with NOAA-18 using changes in inclination, RAAN, and altitude. Then in phase four, OSCAR will perform R-bar hops and enter a natural circumnavigation to inspect NOAA-18. After the inspection, OSCAR will dock to NOAA-18 using the MEV-1 method shown. In phase five, OSCAR will replace NOAA-18's batteries and S-Band transmitter using seven different tools. OSCAR's modules are shown in CAD models with specific components relating to propulsion, power, communications, docking, and the GITAI inchworm robot arms highlighted. Specific dates for each phase are also shown at the bottom, with the mission ending in phase seven. During phase seven, OSCAR will either start a new mission or move to a graveyard orbit.

II. Mission Design

A. OSCAR Spacecraft Overview

OSCAR consists of two mission modules launched as separate payloads. The first is the propulsion unit, Asterix. The second is the payload unit, Obelix. Asterix holds OSCAR's main propulsion system, power supply, and the master On-Board Computer (OBC), as well as an independent Attitude Determination And Control System (ADACS) and independent thermal control units. Obelix holds subsystems necessary for the mission, which include four manipulators for on-orbit servicing, a storage drum containing the client's replacement components, remote sensing instruments for inspection missions, and a dependent OBC to maintain coasting conditions prior to unification. Obelix also includes a smaller independent ADACS and an independent thermal control system, as well as a primary (non-rechargeable) battery to allow Obelix to coast and maintain attitude prior to unification with Asterix, at which point Asterix will provide power and control for Obelix. Unification occurs 7 days after separation from the launch vehicle, following SpaceX's rules for Rideshare users [2].

A trade study was conducted to determine the most suitable launch architecture for OSCAR, evaluating five criteria with an emphasis on cost and reliability. Reliability was characterized using historical success rates with an Eulerian smoothing factor to account for small data samples.

A system consisting of two separate modules that combine after launch vehicle separation was chosen to save launch costs, as OSCAR's mission requires a mass and size that exceeds the envelope for a single Falcon 9 XL plate, and therefore would necessitate a Cake Topper configuration if launched as a single system. The Cake Topper configuration would significantly increase launch costs from $7.3 M to $25 M (approximation, as SpaceX does not guarantee Cake Topper pricing from the SpaceX Rideshare pricing calculator) [3].

The SpaceX Rideshare program [3] was selected due to its higher effective reliability and greater payload accommodations when compared to other programs such as ESPAStar-D. This choice also gave design constraints so OSCAR would comply with its payload user guide. These constraints led to requirements for OSCAR related to structural loads, vibrational environments, and interfaces. OSCAR is designed to use two Falcon 9 XL plates for a launch cost of $3.2 M for Asterix and $4.1 M for Obelix.

Obelix is responsible for managing the servicing hardware used during in orbit operations. Figure 2 shows the Obelix CAD model, with identified key features. Its primary objectives are to store replacement components and to interface with other OSCAR subsystems and the client satellite itself. Obelix is a rectangular structure with a chamfered upper geometry to meet the launch vehicle's volume constraints. The majority of its internal volume is occupied by the replacement part drum. For the given example mission, this drum holds a full set of batteries for the NOAA-18.

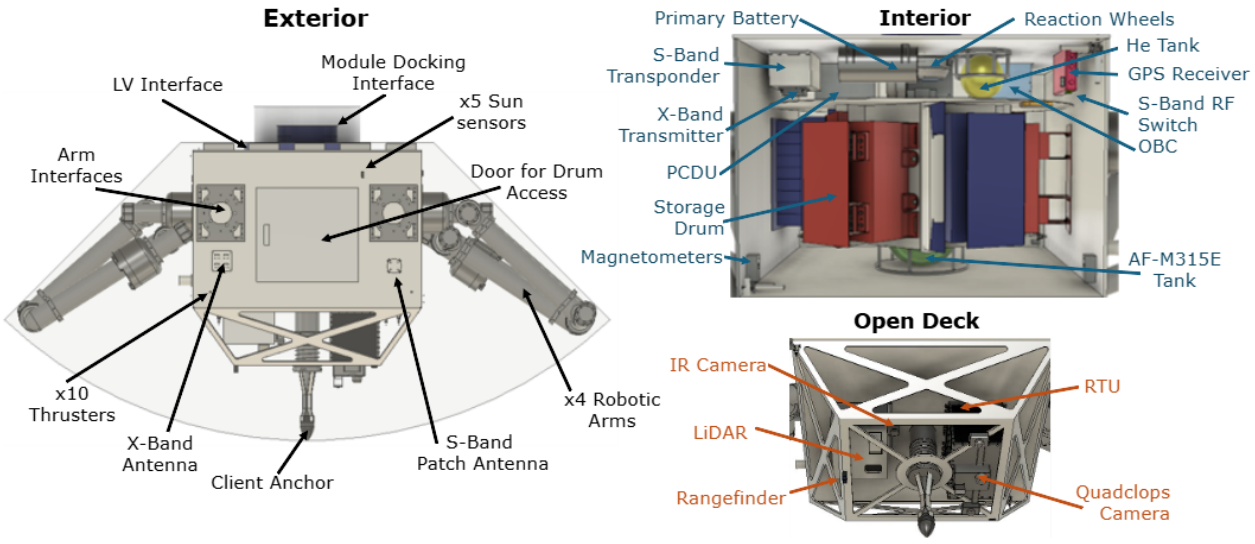

Fig. 2 Obelix CAD Model. The exterior of the payload module (left) is shown inside the Rideshare volume with key components pointed out. The interior of the module (top right) hosts the replacement component drum as well as GNC, CCE, and propulsion components. The open deck (bottom right) hosts the majority of the inspection equipment.

The exterior of Obelix has multiple interface ports to enable servicing arms to change positions and access different sides of a client. The module also contains the ADACS and communications hardware required for mission objectives. The module also contains green propellant thrusters for fine maneuvering. However, the bulk of propulsion is supplied by OSCAR's second module.

Asterix is the propulsion module of OSCAR, responsible for storing the fuel tanks used for rendezvous, docking, and maneuvering. In addition to housing the fuel tanks, Asterix contains a toolbox with uniquely designed instruments for battery replacement. These tools are arranged so that the robotic arm can easily attach to them using its end effector and return them to the toolbox after use.

Asterix also houses several critical GNC components, including star trackers, a gyroscope, magnetorquers, and other sensors and actuators to maintain accuracy and situational awareness, as shown in Tables 12 and 13. The module has a generally cube-like shape, with a docking mechanism perpendicular to its solar panels, allowing it to dock and connect with Obelix. Asterix is shown and labeled in Figure 3.

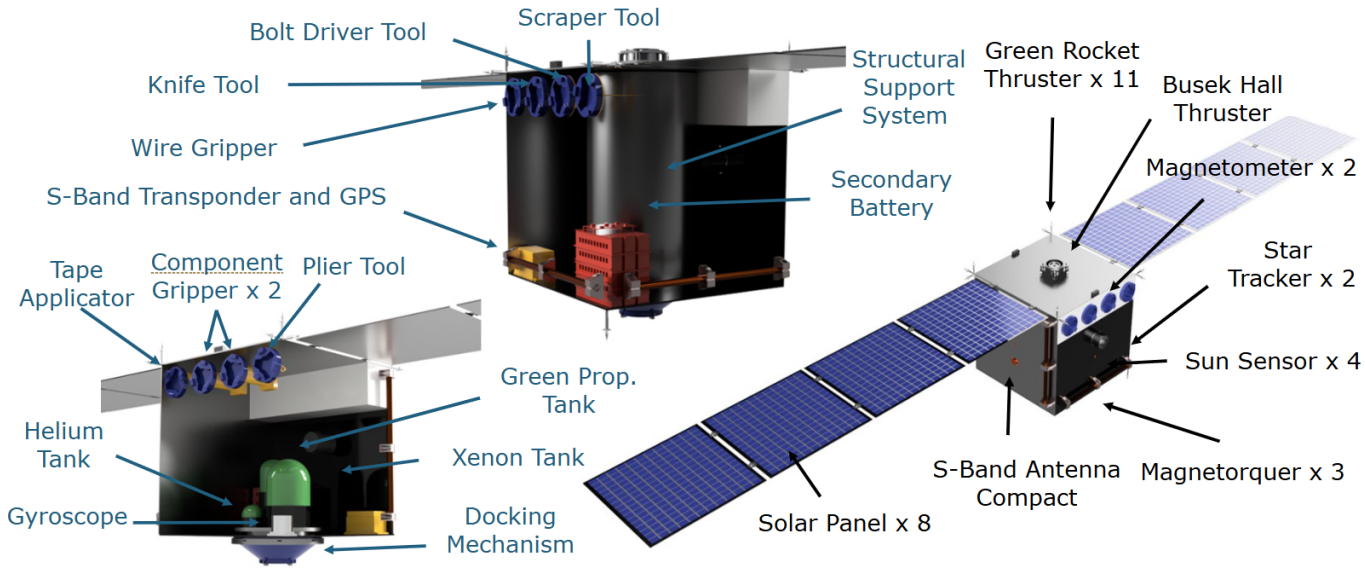

Fig. 3 Asterix CAD Model. The exterior of Asterix is shown on the right with key components labeled. Interior views are displayed at the bottom left and top of the image, highlighting tools used for battery replacement, fuel tanks, sensors, and other components.

The Asterix and Obelix modules are unified using a rigid docking interface inspired by the Gemini-Agena docking system, shown in Figure 4. The female docking port on Obelix and the corresponding male port on Asterix combine to provide a structurally secure connection between the two. Upon docking, power and data transfer are established through four internal contact points. This architecture allows the two modules to function as a unified spacecraft while still meeting SpaceX's specifications on volume and mass of a single payload.

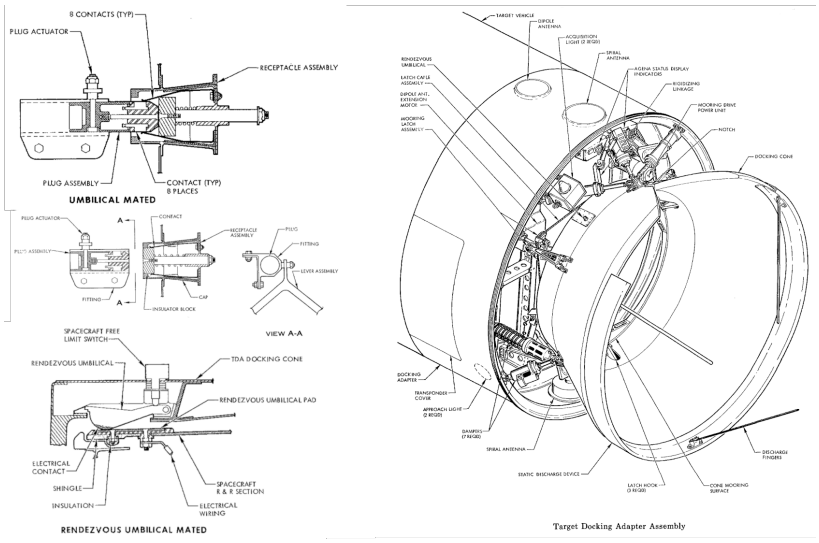

Fig. 4 Gemini-Agena Docking Male/Female Interface and Latches. Four latches distributed around the Gemini male cone mate with female counterparts and provide data and power interchange. The dock is controlled and guided with dampers and mooring assists on the female Gemini port [4].

B. Structural Analysis

Asterix and Obelix must also survive the vibrational loads expected during launch. To address these load cases, a material trade study was conducted to identify materials suitable for mission requirements. Following this, finite element analysis (FEA) of the modal response and maximum thruster load cases was performed. The results were used to help define the structural design and final material selection.

A titanium alloy and two aluminum alloys were evaluated as potential candidates for the spacecraft. The materials were compared based on ultimate tensile strength, fatigue strength, Young's modulus, machinability, and density. The aluminum alloys considered were 6061 and 7075, while the titanium alloy was Ti-6Al-4V. The corresponding material properties are listed in Table 1.

Table 1 Materials Considered for Main Structure. Two aluminum alloys were considered along with a titanium alloy for the main structure of the spacecraft.

Material	Density (g/cm^3)	UTS (MPa)	Y Modulus (GPa)	Fatigue (MPa)	Machinability (%)
Aluminum 6061 [5]	2.7	310	69	96	100 [6]
Aluminum 7075 [5]	3	560	70	160	65 [6]
Titanium 6Al-4V [5]	4.4	1000	110	600	25 [7]

Using modal analysis, shown in Figure 5, the natural frequencies of both Asterix and Obelix were determined to be greater than 40 Hz, which satisfies the requirement for the SpaceX Rideshare Program [3]. Asterix's lowest mode shape had a frequency of 70 Hz, while Obelix's lowest mode shape was 51 Hz when using Aluminum 6061. Using Aluminum 7075 resulted in lower frequencies of 68 Hz for Asterix and 47 Hz for Obelix. The titanium alloy produced frequencies comparable to Aluminum 6061, at 69 Hz and 50 Hz, respectively.

Aluminum 6061 was ultimately chosen due to its lower density compared to titanium alloys. Although the resulting natural frequencies are comparable, this is primarily achieved through the higher stiffness of titanium. Ultimately, reducing the spacecraft mass decreases the required fuel, making Aluminum 6061 the preferred choice. Additionally, aluminum is easier and more cost-effective to manufacture.

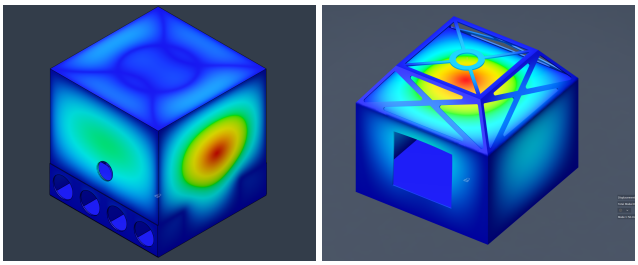

(a) Asterix **(b)** Obelix

Fig. 5 Modal Analysis. This figure shows the first mode shape of both Asterix and Obelix using Aluminum 6061 during modal analysis. Asterix's first mode shape causes the walls of the spacecraft to flex in and out. Obelix's first mode shape causes the top of the spacecraft to flex in and out.

The launch loads are provided on the basis of a range of natural frequencies and the mass of the spacecraft. The mass of Asterix is 377.59 kg, and the mass of Obelix is 576.25 kg. This puts the two spacecraft under different launch load conditions. The launch load conditions for each are listed in Table 2.

Table 2 Launch Loads. A summary of the expected launch loads for both modules is provided.

Vehicle	Axial Load (g)	Lateral Load (g)
Obelix [5]	2	10.5
Asterix [5]	2.5	11

C. Trajectory Requirements

1. Guidance, Navigation, and Control

The mission trajectory is designed to enable safe, fuel-efficient rendezvous, servicing, and inspection operations across multiple client satellites while satisfying launch vehicle constraints and on-orbit safety requirements. The trajectory architecture is divided into sequential mission phases, including post launch separation, module unification, orbit transfer and phasing, proximity operations, docking, and subsequent transfer to secondary inspection targets.

Following deployment via the Falcon 9 rideshare, the Asterix and Obelix modules are inserted into similar initial orbits and maintain safe separation in accordance with rideshare constraints. A mandatory waiting period of seven days is observed prior to any proximity operations to comply with launch provider requirements and to ensure safe dispersion from other passenger payloads [3]. After this period, the two modules perform a controlled rendezvous and docking maneuver to form the unified OSCAR spacecraft. STK was used to propagate orbits and simulate orbital maneuvers throughout the mission [8].

Once unified, the spacecraft first performs a 0.98° inclination change. Then OSCAR coasts until the Right Ascension of Ascending Node (RAAN) is slightly below NOAA-18's RAAN. OSCAR uses J2 perturbation to precess RAAN by 39.6°. OSCAR then performs a burn to increase altitude by 361.3 km to match NOAA-18. These maneuvers are used to match the orbital parameters of OSCAR to the client satellite and minimize propellant usage by leveraging natural orbital dynamics. In particular, the use of J2 perturbation-driven RAAN precession allows OSCAR to gradually align its orbital plane with the target without requiring large, costly plane change maneuvers.

Once the spacecraft is within close proximity of the first client, NOAA-18, operations transition into a Radial Bar (R-Bar) approach in which the spacecraft approaches the client along the radial direction from Earth. An R-Bar approach is chosen because it prioritizes the safety of OSCAR and the client satellite. In case of a loss of control, the R-Bar will ensure OSCAR drifts away from the client satellite. From the rendezvous, OSCAR arrives 700 m below NOAA-18, then performs 3 R-Bar hops to approach the client satellite. Each hop will allow OSCAR to check that all systems are operational during approach. After the R-Bar hops, OSCAR is 100 m below NOAA-18. OSCAR then enters into a Natural Motion Circumnavigation (NMC) around NOAA-18. This approach allows OSCAR to view NOAA-18 from multiple angles while minimizing the amount of Δv used for inspection. After completing two NMCs around NOAA-18 OSCAR will be back on the R-Bar. Then, OSCAR will approach NOAA-18 at 3.64 cm/s, eventually docking with

NOAA-18. OSCAR will stay docked to NOAA-18 for five days for servicing. After servicing, OSCAR will detach and move away from NOAA-18 along the R-Bar. The results of the Δv budget analysis for these maneuvers is shown in Table 3.

Table 3 NOAA-18 Rendezvous, Docking, and Inspection Maneuvers. A summary of the Δv required for inclination, RAAN, and altitude changes to rendezvous and dock with NOAA-18 is provided.

Maneuver	Δv (m/s)	Time (days)
Inclination Change	206.9	311.3
RAAN Precession	0	33.9
Altitude Change	85.3	23.5
Inspection and Docking	12.9	5.1
Total	**305.1**	**373.8**

There are two major risk vectors involved in OSCAR's mission. The first is the risk of docking failure, for both the unification of Asterix and Obelix, and for OSCAR's docking with the client. This risk was simulated with a Monte Carlo simulation with varying random perturbations and RCS imperfections to derive safe approach and capture velocities of 14 cm/s and 5 cm/s for unification and client dock, shown in Figure 6. The second risk vector is uncertainty in both OSCAR's position and the target's position. This was quantified using a Mahalanobis covariance distance matrix using direct ground station ephemeris data augmented with sensor variance vectors built using component precision values. At a 5-σ (6×10^{-5}%) risk margin, inspection would be performed at a radial distance of 16 m from the client. The modeled approach speed of 3.64 cm/s is within the safety margin for docking.

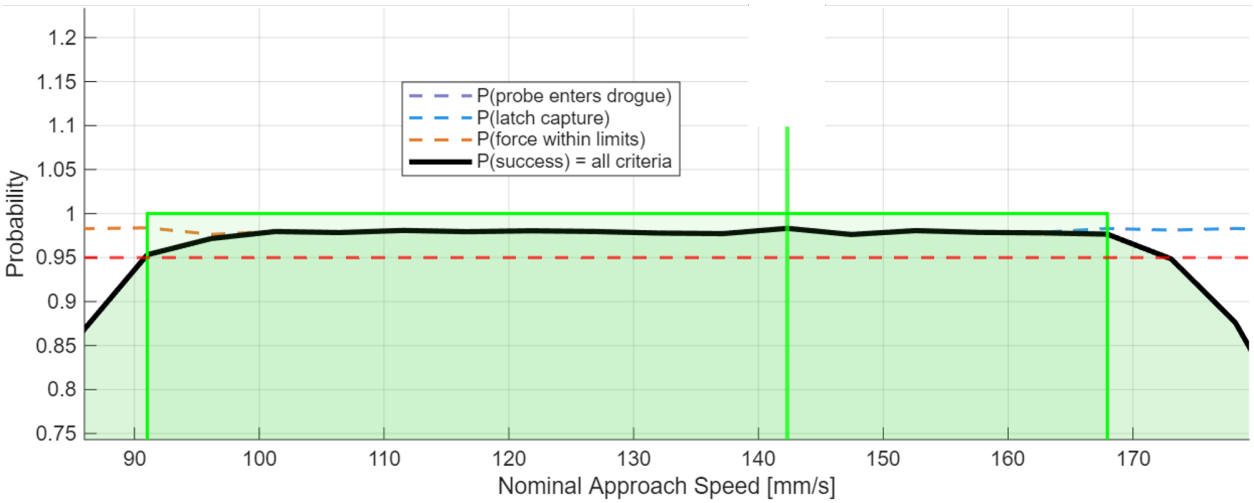

Fig. 6 Cooperative Docking. Monte Carlo simulations found an approach and capture speed of 14.2 cm/s to be the safest for Asterix's and Obelix's unification maneuver.

After servicing NOAA-18, OSCAR will rendezvous and inspect Landsat-8 and Landsat-9. J2 perturbation was used to change RAAN for Landsat-8 and Landsat-9 rendezvous. For J2 perturbation to be effective, the orbital altitude is changed from the client satellite. The orbital altitude is increased by 200 km above that of Landsat-8. OSCAR coasts until RAAN precesses by 173.3°. Then, OSCAR performs a burn to match altitude with Landsat-8 while also matching in-track and cross-track components. OSCAR is then on the R-Bar and follows a similar inspection process to NOAA-18. Landsat-8 will not include a docking sequence. However, a close inspection will be included where OSCAR will approach on the R-Bar and perform an NMC close to the target to inspect Landsat-8's surface. Using 13.0 m/s of Δv for inspection, OSCAR will stay in an NMC for a far inspection for one day and an NMC close inspection for three days.

After inspection of Landsat-8, OSCAR will rendezvous and inspect Landsat-9. OSCAR will decrease altitude by 50 km and use J2 perturbations to precess RAAN by 4.1°. Then, OSCAR will raise orbital altitude back up to Landsat-8. An additional Δv is required to match in-track between OSCAR and Landsat-9. The inspection process used with

Landsat-8 will be used with Landsat-9. Using another 13.0 m/s of Δv for inspection, OSCAR will stay in an NMC far inspection for one day and an NMC close inspection for three days. The Δv budget for these maneuvers is shown in Table 4.

Table 4 Landsat-8 and 9 Rendezvous, Docking, and Inspection Maneuvers. A summary of the Δv required for inclination, RAAN, and altitude changes to rendezvous and inspect Landsat-8 and 9 is provided.

Maneuver	Δv (m/s)	Time (days)
Landsat-8 Altitude Change	68.4	9.5
Landsat-8 RAAN Precession	0	189.1
Landsat-8 Altitude Match	182.5	30.5
Landsat-8 Inspection	13.0	4.0
Landsat-9 Altitude Change	27.1	3.3
Landsat-9 RAAN Precession	0	4.1
Landsat-9 Altitude Match	310.0	51.8
Landsat-9 Inspection	13.0	4.0
Total	**614.0**	**296.3**

After the mission is complete, OSCAR will de-orbit to promote sustainability. The total mission time is 1.83 years using a total Δv of 893 m/s for electric propulsion, and 38.9 m/s for proximity operations.

2. Propulsion

The propulsion requirement is a quantitative mission requirement tied directly to the selected propulsion hardware and mission thrust needs. The spacecraft propulsion subsystem shall provide sufficient mission Δv and thrust authority to support rendezvous and proximity operations for the designated client spacecraft, including a minimum total Δv capability of 893 m/s.

Table 5 Selected Propulsion Subsystem Components. The table shows the selected propulsion components, item code, and their performance characteristics.

Component Type	Component Chosen	Performance	Output	Mass	Power
Hall Effect Thruster	Busek BHT-1500 (Xe) [9]	1865 s	0.179 N	6.6 kg	2700 W
RCS Thruster	Aerojet Rocketdyne GR-1 (AF-M315E) [10]	235 s, 8 mN-s	1.1 N	0.33 kg	22 W
Xenon Tank	96 L Capsule COPV Tank & Xenon [11]	—	—	114 kg	—
AF-M315E Tank	2×19 L Capsule COPV Tank & AF-M315E [11]	—	—	35.5 kg	—
Helium Tank	2×3 L Spherical COPV Tank & Helium [11]	—	—	1.3 kg	—

The selected propulsion architecture consists of a Busek BHT-1500 Hall effect thruster using xenon as the primary high-efficiency propulsion device, an Aerojet Rocketdyne GR-1 thruster using AF-M315E for reaction control and proximity operations, and dedicated storage tanks of xenon, AF-M315E, and helium, as shown in Table 5. This combination was selected to separate the mission propulsion function into two regimes: efficient, high-specific-impulse thrust for rendezvous and large translational maneuvers, and higher-thrust chemical control authority for docking, close-range translation, and safety separation maneuvers.

The minimum rendezvous thrust requirement is 29 mN. The selected Hall effect thruster produces 179 mN, which provides a rendezvous thrust margin of 150 mN or 517.2% [9]. This result shows that the Hall effect thruster exceeds the minimum rendezvous thrust requirement by a substantial margin and is therefore suitable for the low-thrust orbit-matching and approach phases required for NOAA-18 servicing and for Landsat-8/Landsat-9 inspection transfers.

The minimum proximity operations thrust requirement is 2 N. With a GR-1 thruster producing 1.1 N, at least two GR-1 thrusters must be available on each axis for proximity maneuvers, which yields 2.2 N and a corresponding thrust margin of 0.2 N or 10% [10]. Thus, a two-thruster GR-1 firing case satisfies the minimum proximity operations thrust requirement for close-range translation, docking corrections, and collision-avoidance maneuvers.

The mission Δv requirements are driven primarily by a minimum total Δv capability of 893 m/s, and with a 20% growth allowance, a Δv of 1.1 km/s is used for calculations. For proximity operations, a 100 m/s is reserved. Within this architecture, the xenon-fed Hall thruster serves as the primary source of efficient mission Δv, while the AF-M315E reaction control system provides the rapid-response thrust needed during final approach and close-proximity operations. Accordingly, the propulsion subsystem configuration is consistent with the required mission split between high-efficiency rendezvous maneuvers and higher-thrust proximity operations.

Propellant mass was estimated using the Tsiolkovsky rocket equation,

$$m_p = m_0 \left(1 - e^{-\Delta v/(g_0 I_{sp})}\right) \tag{1}$$

where m_p is the required propellant mass, m_0 is the spacecraft mass at the start of the maneuver sequence, $g_0 = 9.81$ m/s^2, and I_{sp} is the specific impulse of the propulsion device. For the xenon-fed Hall effect thruster, using $\Delta v = 1.1$ km/s, $I_{sp} = 1865$ s, and $m_0 = 1300$ kg, which gives a xenon propellant mass of 76 kg [9]. For the proximity operations system, using AF-M315E with $\Delta v = 100$ m/s, $I_{sp} = 235$ s, and $m_0 = 1300$ kg, which gives an AF-M315E propellant mass of 55 kg [10]. Based on these calculations, the propulsion subsystem uses one 96 L COPV tank for xenon and two 19 L COPV tanks for AF-M315E. Based on the mass-to-volume ratio of 0.4 of the NASA Dawn COPV tanks, this makes the total fueled tank masses of 114 kg for xenon and 37.5 kg for AF-M315E [11].

Helium is used as the pressurant for the AF-M315E propulsion system in order to maintain positive tank pressure and ensure reliable propellant expulsion as the monopropellant is depleted. In this configuration, two 3 L helium tanks store a total of 0.3 kg of helium, which is carried separately from the AF-M315E propellant mass budget. Because the helium functions only as a pressurant and does not contribute directly to thrust production, it is accounted for as a supporting consumable within the propulsion subsystem rather than as mission Δv propellant.

Based on the selected thrust levels, the propulsion subsystem satisfies the minimum thrust requirements for both rendezvous and proximity operations. The selected architecture is appropriately matched to those mission requirements and provides the necessary propulsion functionality for both servicing and inspection operations.

D. Component Replacement Servicing Mission

1. Docking & Arm Mobility

Once the spacecraft has arrived at the client satellite, it will dock by inserting a probe, located on the forward face of Obelix, into the spent apogee kick motor on NOAA-18 far enough that the distal end of the linkage is past the nozzle throat. Afterwards, the linkage is withdrawn far enough for the inward projections formed on the level spreaders to engage the linkage's recess. The level spreaders are then spread to a predetermined angle to conform to the inner curve of the apogee kick motor's combustion chamber. Further withdrawal of the linkage will then compress the shaft spring, retracting the spreaders and pulling the two spacecraft together. The curvature of the level spreaders conforms to the inner curves of the apogee kick motor, reducing the contact pressure, which, along with careful material selection, practically eliminates the threat of cold welding [12]. This provides a load-bearing dock which, along with stanchions, prevents axial and non-axial relative motion between the two spacecraft. The probe is shown in Figure 7.

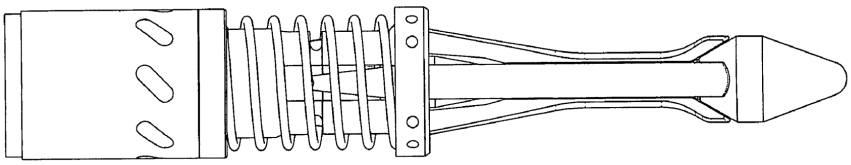

Fig. 7 MEV Style Docking Probe. The conical probe head is made out of an impact-damping material to prevent damage from capture to either the client engine bell or the probe itself. Spreaders are activated via actuators at the base of the probe, and the helical spring retracts to bring the two spacecraft together.

Once the dock is secure, Obelix will use its four robotic manipulators and Asterix's onboard toolkit to carry out the battery and transmitter replacement procedures. The GITAI Inch Worm Robot was selected as the robotic arm for Obelix [13]. It is a COTS, space-rated robotic manipulator, and it has the unique feature of being equipped with connection ports on both ends. This allows the arm to traverse the spacecraft via an array of connection points located

around Obelix. Each arm is equipped with cameras on both ends for AI recognition and fiducial markers detection. A drawing of the robotic arm can be seen below in Figure 8.

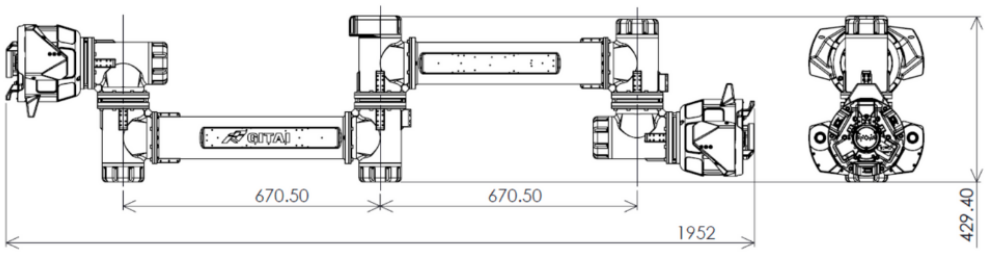

Fig. 8 Drawing of GITAI Inch Worm Robot [14]. A COTS, inchworm-style robotic arm that has been previously tested on the International Space Station. The GITAI robot arm has connection ports on each end, allowing it to maneuver between connection ports.

2. Tools

OSCAR is equipped with seven unique tools for component replacement that are located on Asterix: a bolt driver for removing retaining bolts, a multi-purpose gripper with two sets of claws for securing wires and Multi-Layer Insulation (MLI), an ultrasonic knife for cutting MLI, a scraper for removing residual adhesive after battery removal, a tape applicator for repairing the MLI after the replacement is complete, a two identical gecko style gripper for handling batteries, and a specialized plier tool for removing mil-spec power connectors. All eight tools, while designed for this mission, are versatile enough to be useful in any mission involving external component replacement. Each tool will have a unique fiducial marker label for the autonomous AI system.

An ultrasonic, vibrating knife was chosen for removing MLI to allow for easier and more precise cutting with minimal force applied. Static cutting tools would require more pressure and provide less consistent cuts, and rotating cutting tools would be harder to control and be rougher on the MLI, which we plan to reuse. A NASA-style gecko gripper is used to pick up and place components during repair. Four space-grade gecko grippers are merged into one tool to be able to support around 95 kg [15]. The NOAA-L 8-cell battery packs and 9-cell battery packs weigh 20 and 22 kg, respectively [16]. The grippers work by using a mechanical system that can stick and unstick to surfaces without the use of adhesives [15]. A tool to apply MLI tape has been designed specifically for the mission. The tape applicator models a tape runner, a common tool used for scrapbooking, while allowing the robot arms to provide the needed pressure. The ultrasonic knife will be used to cut the tape once the desired length is reached.

3. Battery Replacement Procedure

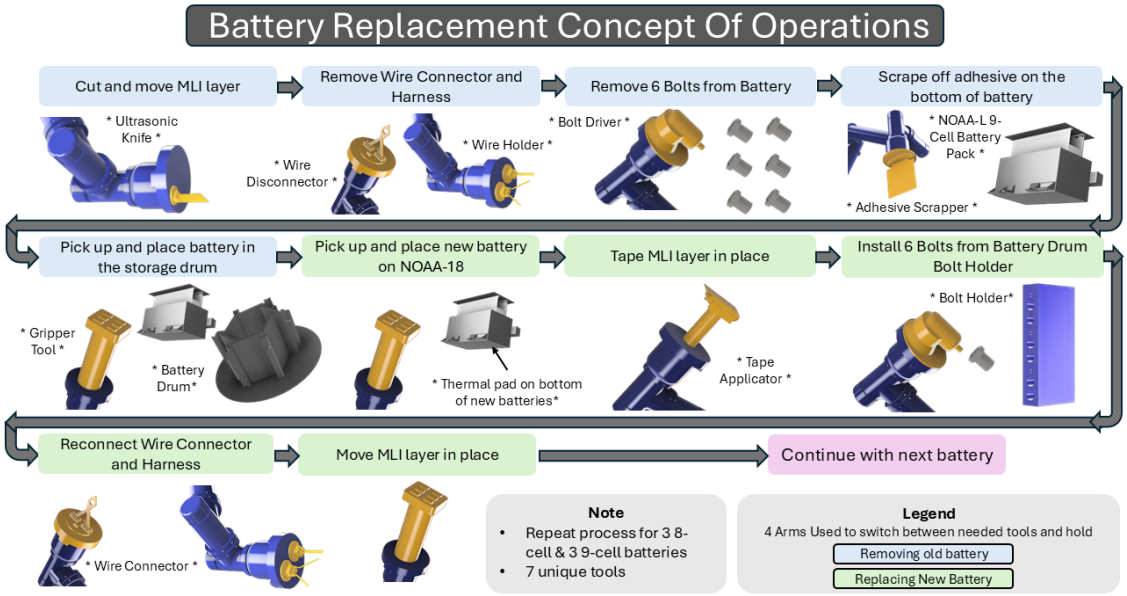

Fig. 9 NOAA-18 Battery Replacement Procedure. The procedure includes seven different tools: ultrasonic knife, wire disconnecter, wire holder, bolt driver, adhesive scrapper, gripper, and tape applicator. The light blue sections show the battery removal procedure, and the light green sections show the replacement procedure. This process will be repeated with three 8-cell batteries and three 9-cell batteries.

The battery replacement procedure requires six new bolts for each of the six new batteries. The new bolts will be threaded into the bolt holder shown in the battery replacement CONOPS in Figure 9. The bolt holder will be housed with the new batteries and S-Band transmitter in the battery storage drum, which is held within the Obelix module. An actuator is used to rotate the drum, allowing the arms to reach all the batteries in the circular-style drum. NOAA-18 has 8-cell and 9-cell battery packs in pairs [16], so the battery drum alternates the batteries to allow for easy access. Additionally, the tools are stored on the walls of the Asterix module, also allowing the arms to easily access them.

To start the replacement procedure, an arm will attach to the ultrasonic knife and cut the MLI layer that sits on top of the NOAA-18 batteries. The gripper tool will be used to pull off the MLI layer, providing access to the batteries. The wire disconnecter tool will then remove the military connector, removing the wire harness to the battery and placing it in the wire holder tool. The bolt driver will then be used to remove six bolts securing the battery to the client. Following this, the adhesive scrapper will be used to remove the battery from the client. This battery will be picked up by the gripper tool and placed in the replacement battery's spot within the battery drum. It will be secured to the drum using two bolts.

The replacement battery will be placed on NOAA-18 and secured using the bolts brought with OSCAR. Since applying adhesive to the new batteries during the mission is not feasible, a pre-connected thermal pad will be placed on the bottom of the new batteries. The thermal pad provides the same functions as the adhesive on NOAA-18. The thermal pad will ensure that the heat from battery charging and discharging will be uniformly dissipated. After the replacement battery is secured, the MLI will be replaced on the client and sealed using the tape applicator tool. The battery drum will then spin 60° so the arms can access the next replacement battery. This process will be repeated with each of the six batteries.

A similar process will be followed to remove and replace the S-Band transmitter. Using the same tools and capabilities of the robot arms, external component replacement of most kinds could be completed, allowing for similar missions to be carried out.

E. Communications and Inspection Servicing Mission

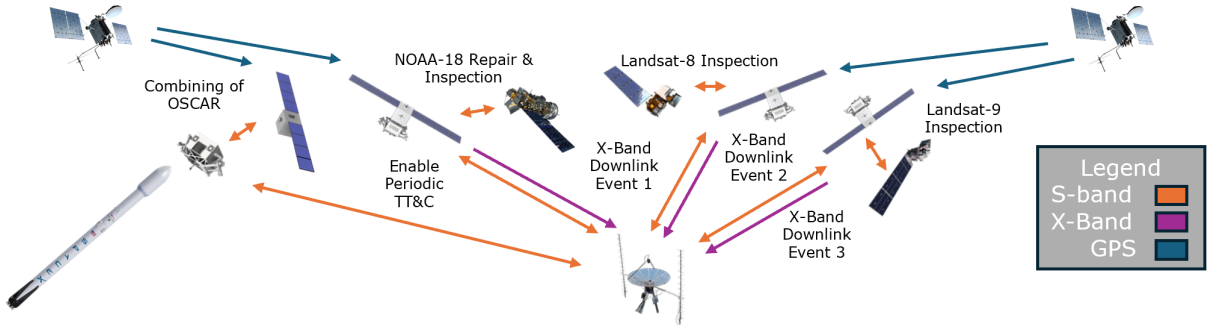

Fig. 10 Communication CONOPS. The communications and inspection concept of operations outlines the mission activities undertaken by OSCAR from launch to servicing and inspection. Asterix and Obelix will join together in orbit and then conduct their rendezvous with NOAA-18. Once the service activities have been completed, OSCAR will conduct inspections of Landsat-8 and Landsat-9 satellites, communicating high-data-rate inspection information of 20 to 25 mbps to Earth using the X-band link.

The communications, command, and environment system stores, modulates, and handles data transmissions. The system enables the OSCAR spacecraft to receive uplinks, transmit downlinks, and perform cross-links between the client satellites. S-band, X-band, and GPS are the three communication sub-systems. The system uses the idea of supervised autonomy and should not need command data for mission updates in real time, but should downlink critical data periodically. Three On Board Computers, referred to as OBC's, are used on OSCAR with the Constellation OBC on Asterix and the Amethyst OBC on Obelix [17] [18]. Obelix will house most of the communication and ADACS system, including a remote terminal unit as well as the OBC [19]. Mission requirements were the drivers for down-selecting the specific frequency bands used. The OSCAR spacecraft must be able to receive and transmit telemetry, tracking, and command data, also referred to as TT&C, directly with the ground station, cross-link with client satellites, and downlink data rates between 20 and 25 Mbps after inspection data is collected. The maximum allowable pointing offset angle is 3° and the minimum elevation angle from our ground station will be 10° to maintain link quality.

With these requirements in mind, S-Band was chosen since it matches the systems used on all three clients in which cross-link is necessary [20] [21] [22]. The S-Band system uses an L3Harris C/TT-520 transponder with an internal diplexer to receive and transmit TT&C data supporting an uplink of 4 kbps and a downlink of 8 kpbs [23]. TT&C data will be down-linked every one to five seconds for the duration of the mission [24]. The position, navigation, and timing data will also be down-linked every one second [25]. S-Band will also be used to downlink health and status data with specific failure modes during the combination of the Obelix and Asterix modules, as well as the docking with NOAA-18. If any failure modes are realized during the OSCAR module combination, the mission will be aborted, and if docking failure modes are realized, the repair phase will be aborted. S-Band will also be used for a data rate of 8 kbps of cross-link while approaching each client. The rest of the S-band system includes two hemispherical omnidirectional antennas and an RF switch for continuity. The S-Band antennas used are the STT-System Technik GmbH S2023 Circular Antenna and the Anywaves Compact Antenna *Space Mission Analysis and Design* [26]

X-band was selected as the high data rate system to downlink the inspection data. This system includes the CAVU X-Band Transmitter and a Printech X-Band 4x4 Patch Array Antenna [27][28]. The Printech X-Band 4x4 Patch Array Antenna peak antenna gain is 16.7 dBi derived from equations in *Space Mission Analysis and Design* [26]. The X-Band system matches the needed data rates for the mission while having the least attenuation when compared to high RF bandwidths[29]. Both the X-band and S-band systems described will be housed on Obelix. The inspection data will be downlinked via X-band on 03/11/2030, 10/04/2030, and 10/15/2030. An additional S-band L3Harris C/TT-520 transponder and Anywaves Compact Antenna will be housed on Asterix for communication before the combination of the two modules is completed. Both the OSCAR modules will also include a separate PolaRx5 GNSS Receiver for position, navigation, and timing data [30].

The ground station was selected when considering a cost-saving constraint. Instead of building a ground station for this specific mission, NASA's NSN McMurdo ground station will be used to receive and transmit mission data for

OSCAR [31]. McMurdo ground station is located in Antarctica and is equipped with advanced tracking systems for precise satellite alignment [31]. The McMurdo ground station uses X- and S-band antennas, which are 10 m in diameter, and using a robust power system, is able to continue operations during extreme weather conditions [31]. OSCAR will be able to maintain contact with the ground station because, being in a polar orbit, it will pass over the ground station during the entire duration of the mission. If further missions are completed after the inspection of Landsat-8, we will store and forward the data until another pass over the South Pole is completed.

The communication components down-selections use a right-hand circular polarization to reduce sensitivity while OSCAR rotates [29]. The S-band Circular antenna was also specifically chosen to maintain the link during tumbling. OSCAR's signal-to-noise ratio, given a bit error rate, BER, of 10^{-5}, is below 9.6 dB, which drove the choice for QPSK modulation [26].

Inspections will be performed on NOAA-18, Landsat-8, and Landsat-9 from a distance of 16 m during a natural circumnavigation around each client. NOAA-18 inspection will be performed before docking and repairs to assess the current condition and determine that docking can be achieved safely according to the original mission plan. Landsat-8 and Landsat-9 will receive inspections after NOAA-18's repairs are completed. The OSCAR spacecraft is equipped with a Quadclops four-camera system, the RVS 3000-X Light Detection and Ranging (LiDAR), and the modified Boson 640 IR camera to collect still images, LiDAR 3D maps, and IR videos, respectively. This image will be downlinked at a data rate between 20 and 25 Mbps.

The RVS 3000-X LiDAR system will support rendezvous and proximity operations. It was chosen because it is designed for operation with non-cooperative targets such as NOAA-18. Having a field of view (FOV) of 40° allows it to view the entire satellite during proximity operations [32]. DLEM17 and a NASA modified Boson 640 IR camera were chosen because of their low SWaP cost. Quadclops covers all ranges of visual inspection required for the mission. The center camera used for close high-resolution images has an FOV of 4.2° and a focal length of 100 mm. Another camera useful for taking pictures during approach has an FOV of 16.9° and a focal length of 25 mm. The last camera on Quadclops is useful for finding the target during a far approach. The camera has an FOV of 58.7° and a focal length of 6 mm. These four systems will provide accurate information about the client satellite for inspection and during critical proximity operations [33].

F. Power and Thermal Requirements

1. Power

For power, the driving power requirement is a quantitative end-of-life requirement tied directly to the selected power subsystem hardware. The spacecraft's electrical power subsystem shall provide a minimum end-of-life, such that the spacecraft can support loads up to approximately 3450 W through combined operations.

Table 6 Selected Power Subsystem Components. This table shows the different selected power components, their performance characteristics, and footprint.

Component Type	Component Chosen	Performance	Output	Mass	Footprint
Primary Battery	Eagle Picher EAP-12325 [34]	353 Wh	920 W	5.6 kg	740 cm^3
Secondary Battery	GS Yuasa MA190-107 [35]	5001 Wh	2950 W	37 kg	30300 cm^3
Solar Panel	Spectrolab XTE-SF [36] (10.4 m^2)	435 W/m^2	4520 W	1.76 kg/m^2	22 mm

The selected power architecture consists of a Spectrolab XTE-SF solar array, a GS Yuasa MA190-107 lithium-ion secondary battery, and an Eagle Picher EAP-12325 Ag-Zn primary battery, as shown in Table 6. The solar array provides an end-of-life output of 3590 W, which is sufficient to support the highest average operational mode identified in the mission power budget [36]. For servicing and inspection operations, the worst-case average power demand occurs during maneuvering, when the spacecraft requires 2905 W. This condition represents the most demanding continuous operating state, as propulsion, ADACS, thermal control, command and data handling, and supporting communications must all function simultaneously during rendezvous operations.

The use of two different battery types ensures that both Asterix and Obelix remain power self-sufficient during the period between separation from Falcon 9 and docking with one another. The Eagle Picher EAP-12325 Ag-Zn primary battery is a non-rechargeable unit selected to supply Obelix with the required 825 W proximity operations power until it attaches to Asterix [34]. The GS Yuasa MA190-107 Li-ion secondary battery is a rechargeable unit carried by Asterix

to provide continuous power support and energy storage over the full mission lifetime [35]. In addition, the Spectrolab XTE-SF solar array, sized at 8.24 m^2 and producing 3590 W at the end of life, provides sufficient generation capacity to power spacecraft operations while recharging the secondary battery for subsequent eclipse and peak-demand periods [36].

Using the end-of-life solar-array output and the worst-case average maneuvering load, the available continuous power margin is 1620 W. This corresponds to a fractional margin of 24.4%. This margin demonstrates that the solar array alone can support the highest average mission load with a positive end-of-life margin. As a result, the electrical power subsystem is capable of supporting nominal servicing operations for NOAA-18 as well as inspection for Landsat-8 and Landsat-9 while maintaining continuous power to essential avionics and mission subsystems.

Battery performance is driven primarily by eclipse survival and short-duration support for elevated power demand. The secondary battery capacity is 5001 Wh. At the nominal eclipse load of 175 W, the battery-only endurance is 28.6 hr, which is substantially greater than a single low-Earth-orbit eclipse duration and therefore provides ample margin for eclipse survival. Even if the spacecraft were temporarily required to operate at the worst-case maneuvering load using battery power alone, the available endurance would be 1.72 hr. This indicates that the battery system also provides meaningful flexibility for short off-nominal or transitional operating periods.

In addition to average-load compliance, the power subsystem was checked against the estimated maximum transient spacecraft power pull of approximately 2905 W. During sunlit operations, the combined available power from the solar array and secondary battery is 6540 W, which gives a transient peak margin of 3090 W [35] [36]. Thus, the selected electrical power subsystem can support both continuous mission loads and short-duration peak-demand events expected during orbital servicing of NOAA-18 and inspection operations involving Landsat-8 and Landsat-9.

Based on the end-of-life generation capability, available battery energy storage, and peak power support, Requirement P1 is assessed as compliant. The solar array independently supports the worst-case average maneuvering mode, while the battery system provides sufficient stored energy for eclipse survival and sufficient supplemental output for transient peak-demand conditions.

2. Thermal

For thermal, there are a handful of components that have high thermal sensitivity, which are mitigated with active controls, while the majority of components were selected with thermal survivability in mind. The most sensitive thermal component, in terms of range, is the lithium-ion battery, which requires from 10°C to 25°C for operation [35]. Based on industry standards for space vehicles [37], this component required heaters and special handling. There are other thermally sensitive components which come with their own thermal management system, specifically, the RCS thrusters [10] [38], LiDAR [39], and the IR Scanner. Thermal analysis was performed numerically, which estimated the heat load, demonstrating that passive heat rejection was sufficient for maintaining the internal temperature within the overall operating temperature requirements.

$$P_{Thermal} \equiv \sum (1 - \eta_i) P_i \tag{2}$$

Thermal analysis was performed based on the different power modes and estimates for efficiency by component, analyzed for the worst temperature case of all components at 60°C for safety margin. This total heat generated was compared with the Stefan-Boltzmann law for the heat emission of the satellite MLI to see if additional heat rejection was required, such as radiators, which was proven to be unnecessary.

$$P_{Thermal} = A \epsilon \sigma T^4 \tag{3}$$

III. System Summary

This section provides an overview of the key resource allocations and constraints that define the design and feasibility of the overall system. It will go over the mass budget, detailing how mass is distributed across subsystems to meet both structural and launch requirements, as well as the power budget, which evaluates the generation, storage, and consumption of energy necessary for sustained operation. In addition, it outlines the estimated mission cost, offering insight into the financial scope of the development, manufacturing, deployment, and operations. Finally, the major risks associated with the mission are highlighted in the risk matrix, identifying potential challenges and their impacts as well as ways to mitigate or minimize such risks. Together, these elements establish the framework for the overall design and iterative analysis of the Obelix and Asterix systems.

The block diagram shown in Figure 11 shows the two modules that conjoin to become OSCAR. They each start out

as separate spacecraft with their own subsystems, which communicate through RF in the S-band, but after unification, they interface data and power directly, with Obelix slaved to the more powerful OBC on Asterix. Most notable on the block diagram is the specific artificial intelligence system-on-a-chip (SOC), running on the space-rated AI/ML chip, the XQR Versal [40]. Asterix, the propulsion module, holds the main power and propulsion system, with the solar panel array and the BHT-1500 [9], while Obelix, the payload module, stores the payload bay, inspection equipment, which is distributed between AOCS and the payload system, and the robotic arms.

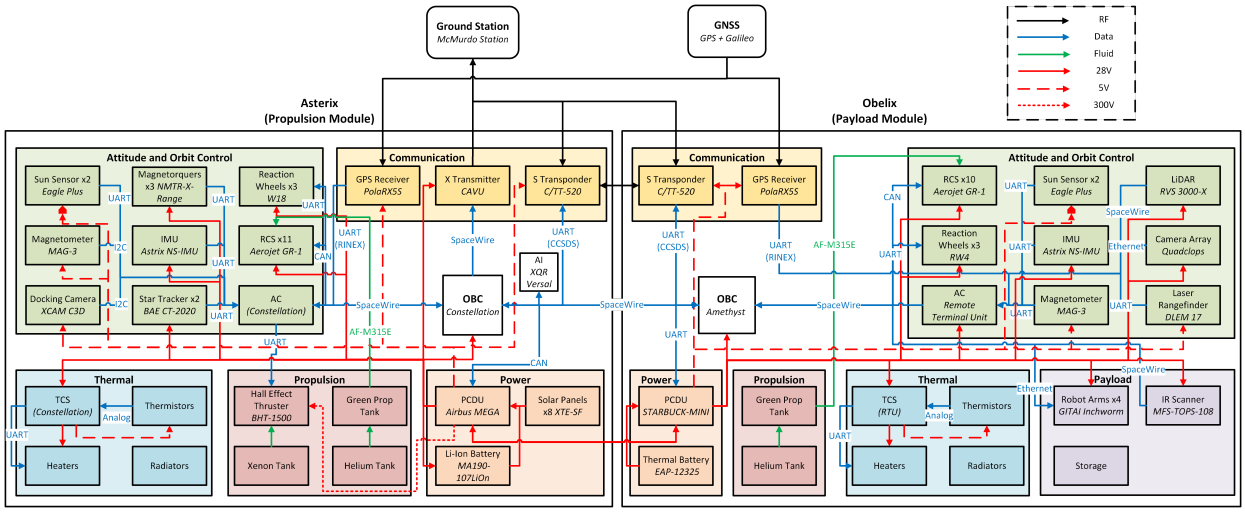

Fig. 11 OSCAR Block Diagram. This diagram illustrates the power, data, and fluid interfaces between the different systems within and between the Asterix and Obelix systems.

A. Mass Budget

The detailed mass budget is listed in the Appendix section in Table 14. The mass budget for Project OSCAR was allocated by the bus selection. As per the user's guide provided by SpaceX [3], the allotted mass per port is 831 kg. The mass of each subsystem and total mass per Asterix/Obelix module are listed in Table 7.

Table 7 Spacecraft Mass Budget. This table shows the mass of each major subsystem, broken down by which module, growth allowance, and upper bound.

Subsystem	Mass (kg)	Asterix (kg)	Obelix (kg)	Growth Allowance	Upper Bound (kg)
Structure	240	97	143	20%	288
Power/Thermal	74	64	10	15%	85
Propulsion	102	60	42	20%	122
Propellant					
Xenon	76	76	0	20%	91
AF-M315E	55	27.5	27.5	20%	66
Communications	8	5	3	20%	10
Control & Command	43	15	28	20%	52
ADACS	21	11	9.6	20%	25
Payload	370	3.5	366	6%	392
Total	**955**	**355**	**600**	—	**1046**

The maximum allowable mass is dependent on the center of gravity relative to the payload origin as outlined by the rideshare user's guide [3]. The mass of the two modules together, along with mass growth in mind, is 1,015 kg.

The majority of this mass is dedicated to the payload, structure, propulsion systems, and fuel storage. The payload is approximately 370 kg between the two modules. The structure is approximately 240 kg between the two modules. The propulsion system is approximately 102 kg between the two modules. Obelix is the heavier of the two modules at 600 kg, while Asterix is the lighter of the two at 355 kg.

B. Power Budget

The fully detailed power budget is shown in the Appendix section in Table 14. The high-level power budget is detailed in Table 8 below. Project OSCAR will operate in five different modes: maneuvering, proximity operations, diagnostics, repair and replace, and eclipse. The most power-consuming mode was maneuvering. The maneuvering mode involves OSCAR traveling from the SpaceX rideshare to the client satellite with the Hall effect, using a majority of this mode's power draw. Repair and replace was the next highest power-consuming mode, with a majority of the power draw coming from operating the arms during component replacement. Proximity operations and diagnostics both occur near the client satellite, with proximity operations being more propulsion-intensive due to maneuvering requirements, while diagnostics is more payload-intensive, focusing on sensor use and data collection. Finally, the eclipse mode is when there is no direct sunlight reaching OSCAR's solar panels, and the main power function is to maintain attitude control.

Table 8 High-level Power Budget by Power Mode, Average Power Draw, and Duty Cycle. Each component's power draw is listed by its use in each of the power modes determined.

	Maneuver		**ProxOps**		**Diagnostics**		**R&R**		**Eclipse**	
Subsystem	**W**	**DC**	**W**	**DC**	**W**	**DC**	**W**	**DC**	**W**	**DC**
Thermal	40	100%	40	100%	40	100%	40	100%	40	100%
Propulsion	2735	100%	607	20%	35	9%	35	9%	0	—
Communications	2	10%	4	20%	10	50%	10	50%	2	10%
ADACS	88	95%	94	100%	94	100%	94	100%	88	95%
Command & Control	25	100%	25	100%	25	100%	25	100%	25	100%
Payload	0	—	47	6%	118	15%	691	90%	0	—
Parasitic	15	—	10	—	10	—	2.5	—	20	—
Total	**2905**	—	**825**	—	**330**	—	**900**	—	**175**	—

C. Cost Budget

The total estimated cost of the mission is $33.07 million based on NASA's PCEC tool [41]. The subsystem costs, along with their respective growth allowances, are shown in Table 9.

The cost distribution highlights that the main share of expenditures goes to the launch and guidance, navigation, and control (GNC) subsystems because of the expenses required for placing a satellite into orbit and the complexity of the guidance and control systems. Subsystems like communications, power, and thermal control make up a smaller part of the cost as a result of the more developed technologies that have been used by aerospace companies, and which have been less prone to risks and uncertainties in this area. The propellant and GNC subsystems had higher growth allowances in order to reduce the costs associated with the high technical complexity of these systems. Payload costs include the costs of the servicing equipment and other components required for particular missions. The growth allowances have been included for all subsystems in order to cover additional costs during development.

D. Risk Analysis

Project OSCAR is an experimental mission that is purely conceptual. The mission carries numerous risks that have the potential to be catastrophic. As such, the risks had to be carefully considered so that preliminary mitigation would lower the chances of these risks causing failure to the mission. The risks of Project OSCAR were compiled into a risk matrix, shown in Figure 12, and plotted with their original values of consequence versus likelihood along with their mitigated values. The risks are associated with the Risk ID column of the Project OSCAR Risk Table. The magnitudes of severity were rated from one to five, with one meaning that the consequence of failure was negligible and five meaning

Table 9 High-Level Mission Cost Estimate. An assessment of the costs of the OSCAR C3 Orbital Servicing mission was done using a subsystem-oriented method. This entailed estimating the cost of each of the subsystems involved and including a growth allowance (GA) to cater for uncertainties during the early stages of design and development.

Subsystem	Cost ($M)	GA (%)	Growth ($M)	Total ($M)
Launch	7.3	0	0	7.3
Project Management	2.5	5	0.1	2.6
Systems Engineering	4.1	10	0.4	4.5
Payload	3.0	20	0.6	3.6
Structures	1.7	5	0.1	1.8
Thermal	0.8	5	0.0	0.8
Power	2.4	10	0.2	2.6
GNC	7.0	15	1.1	8.1
Propulsion	1.9	10	0.2	2.1
Communications	0.5	10	0.1	0.6
CDH	1.9	25	0.5	2.4
Total	**33.1**	**9.9**	**3.3**	**36.3**

that the consequence of failure was catastrophic. If the risk had a lesser than five percent chance of occurring, a score of one was assigned. If the risk had a greater than 50 percent chance of occurring, it was assigned a score of five.

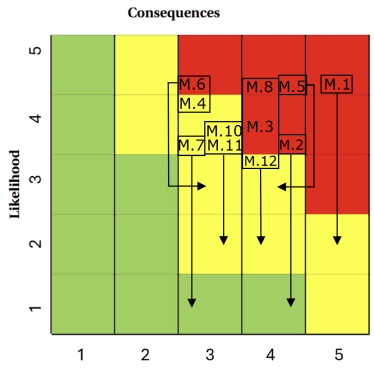

Fig. 12 Risk Mitigation Matrix Summary. The primary risks for Project OSCAR are organized in a 5 × 5 risk matrix. All 11 identified risks have been mitigated from high and medium risk levels down to medium and low levels.

Table 10 Risk Classification Based on Consequence and Likelihood of Failure. Consequence rank was defined via the NASA risk management handbook. Likelihood margins were defined using NASA standards for a class B mission [42]

Consequence of Failure		Likelihood of Failure	
Catastrophic (5)	Total mission failure; failure to satisfy mission requirements.	**Very High (5)**	50%–100%
Critical (4)	Failure to satisfy multiple mission requirements.	**High (4)**	25%–50%
Moderate (3)	Failure to satisfy a mission requirement.	**Medium (3)**	12%–25%
Minor (2)	Mission requirements met; disruption to mission timeline.	**Low (2)**	5%–12%
Negligible (1)	Minimal to no impact on mission outcome.	**Very Low (1)**	0%–5%

For example, M.1 states that if Project OSCAR's satellite enters the client satellite's trajectory for service, there is a potential for the OSCAR modules to collide with the client satellite. It was determined to have a likelihood score of five, meaning it was very likely to happen, and a consequence score of five meaning that if it occurred, it would be mission-ending. To mitigate the likelihood of collision, Project OSCAR is designed to use an R-Bar approach as opposed to a velocity bar approach, which allows OSCAR to never cross the trajectory of the client satellite. This adjusted the likelihood score from five to two, meaning that there was a low chance of failure (between five and twelve percent).

IV. Conclusion

OSCAR, shown in Figure 13, is a modular on-orbit servicing spacecraft designed to extend the operational lifetime of high-value satellites through component replacement and inspection. Using the replacement of degraded batteries on NOAA-18 as a representative mission, this work demonstrates the viability and broader applicability of this technology to existing and future spacecraft.

Feasibility is emphasized through the selection of commercially available, space-rated components and an architecture that is compatible with the chosen Rideshare program. OSCAR's design is supported by analysis such as subsystem trade studies, Δv budgeting, and preliminary structural assessment. These results show that the system can meet mission requirements given by COSMIC and derived from design decisions.

The modular architecture, tool-changing capability, and rotating onboard storage system combine to create an innovative design. These features allow for flexible, repeatable servicing missions with minimal redesign, supporting a wide range of clients. The spacecraft is estimated to cost between $33-36 M and launch on September 15, 2029. OSCAR aims to provide an easily modifiable spacecraft capable of supporting a multitude of clients, demonstrating the viability and impact of on-orbit servicing.

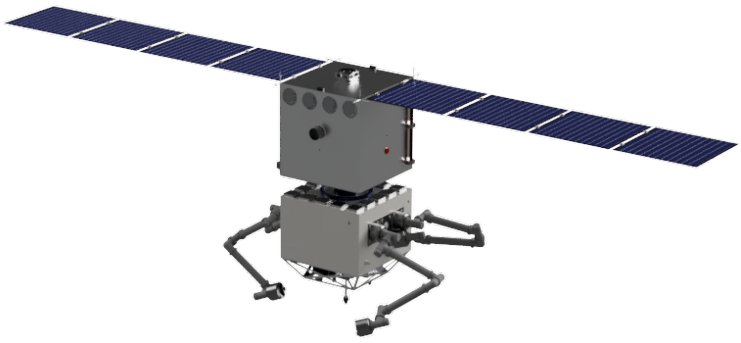

Fig. 13 Full Assembly of OSCAR Spacecraft. OSCAR is a modular on-orbit servicing spacecraft capable of performing replacement and inspection operations on client satellites to restore capability and extend mission timelines.

Appendix

s

A. Guidance Navigation and Control Sensors

Table 11 OSCAR Reaction Wheels Selection. This table shows reaction wheels selected for Obelix and Asterix and their maximum stored momentum.

Actuator and Location	Brand and Type	Momentum (N·m·s)
3 Reaction Wheels on Obelix	Blue Canyon RW4	4
3 Reaction Wheels on Asterix	Bradford W18	18

Table 12 OSCAR Magnetorquer Summary. Selected magnetorquers on Asterix.

Actuator and Location	Brand and Type	Moment (A· m^2)
3 Magnetorquers on Asterix	Taurus NMTR-X-Range	55

Table 13 OSCAR ADACS Sensors. This table shows a list of ADACS sensors, which module they are located on, size, brand, type and accuracy of the sensor.

ADACS Sensor and Location	Brand and Type	Accuracy	Dimensions (mm)
2 Star Trackers on Asterix	BAE Systems CT-2020	1" twist accuracy 1.5" cross accuracy	147 diameter × 305 tall
4 Sun Sensors on Asterix and 5 on Obelix	Needronix Eagle Plus	$< \pm 0.1°$	$29.5 \times 11.5 \times 6.5$
1 Magnetometers on Asterix and 1 on Obelix	AAC Clyde Space MAG-3	$\pm 65\ \mu$T	$35.1 \times 32.3 \times 82.6$
1 Gyroscope on Asterix and 1 on Obelix	Astrix NS-IMU	$< 0.005°$/h Bias $0.0025°/\sqrt{\text{h}}$ ARW	$130 \times 130 \times 117$

B. Detailed Mass Budget

Table 14 Spacecraft Mass Budget. This table is an itemized list of components and their associated item codes, masses and subsystems.

Component	Item Code	Mass (kg)	Subsystem
Solar Panel	Spectrolab XTE-SF	18.3	Power
Hall Effect	Busek BHT-1500	6.6	Propulsion
RCS	Aerojet GR-1 (x21)	6.93	Propulsion
Xenon	Xe-54	76	Propulsion
AF-M315E	$[NH_3OH][NO_3]^-$	55	Propulsion
Helium	He-2	0.6	Propulsion
Xenon tank	Custom COPV	38.5	Propulsion
AF-M315E tank	Custom COPV	20	Propulsion
Helium tank	Custom COPV	2	Propulsion

Table 14 Spacecraft Mass Budget (continued)

Component	Item Code	Mass (kg)	Subsystem
Secondary Battery	MA190-107	42.15	Power
Primary Battery	EAP-12325	5.6	Power
Thermal	Heaters	8	Thermal
Star Tracker	BAE CT-2020 Star Tracker	7.5	AOCS
Sun Sensor	Eagle Plus Digital Dual-axis FSS	0.025	AOCS
Magnetometer	AAC SpaceQuest MAG-3 (x2)	0.024	AOCS
IMU	Astrix NS-IMU	2.72	AOCS
Reaction Wheels A	W18	0	AOCS
Reaction Wheels O	RW4	9.6	AOCS
GPS Receiver	PolaRx5S	0.9	AOCS
Uplink (A)	C/TT-520 S-Band Transponder	0.1	Communications
Downlink (A)	CAVU X-Transmitter	0.07	Communications
Crosslink (O)	C/TT-520 S-Band Transponder	0.1	Communications
Manipulators	GITAI Inch Worm Robot (x4)	200	Payload
Storage	Custom	10	Payload
R&R Batteries	—	125	Payload
LiDAR	RVS 3000-X	15	Payload
Laser Rangefinder	DLEM 17	0.025	Payload
Docking Camera	C3D Camera	0.085	Payload
Wide Camera	Quadclops	3.59	Payload
IR Scanner	Ruggedized Infrared Camera (MFS-TOPS-108)	3.5	Payload
Stanchions	Custom	9	Payload
Scraper	Custom	0.25	Payload
Wire Gripper	Custom	0.25	Payload
Bolt Driver	Custom	2	Payload
Adhesive Applicator	Custom	0.25	Payload
Incision Device	Custom	0.25	Payload
Plier	Custom	0.25	Payload
Unit Gripper	Custom	0.25	Payload
OBC (A)	Constellation	5.4	Command & Control
OBC (O)	Amethyst	3.5	Command & Control
AC (O)	RTU	16.6	Command & Control
AI	DGX Spark	1.2	Command & Control
PDCU (A)	Airbus MEGA PCDU	8.3	Command & Control
PDCU (O)	STARBUCK-MINI	8.3	Command & Control
Dock Port	Gemini-Agena Heritage	20	Structure

C. Power Budget

Table 15 Spacecraft Power Budget by component. The table below breaks down the power supply, duty cycle in %, and average power by operational mode.

Component	Item Code	V	Eclipse		Maneuver		Prox Ops		Diagnostics		Repair	
			DC (%)	Avg (W)	DC (%)	Avg (W)	DC (%)	Avg (W)	DC (%)	Avg (W)	DC (%)	Avg (W)
Solar	Spectrolab XTE-SF	28	100	0	100	-4500	100	-4500	100	-4500	100	-4500
Hall Effect	Busek BHT-1500	300	0	0	100	2700	10	150	1	20	1	20
RCS	Aerojet GR-1 (x21)	28	9	38	9	38	27	112.86	9	37.62	9	37.62
Thermal	Heaters	28	100	300	0	0	0	0	0	0	0	0
Star Tracker	BAE CT-2020 (x2)	28	10	16	10	16	10	16	10	16	10	16
Sun Sensor	Neelix Eagle Plus (x4)	28	0	0	100	2	100	2	100	2	100	2
Magnetometer	AAC Clyde MAG-3 (x2)	5	100	0.2	100	0.2	100	0.2	100	0.2	100	0.2
IMU	Astrix NS-IMU (x2)	5	100	10	100	10	100	10	100	10	100	10
Reaction Wheels	RW4 (x6)	28	5	3	5	3	5	3	5	3	5	3
GPS Receiver	PolaRx5S	5	100	4.7	100	4.7	100	4.7	100	4.7	100	4.7
Uplink	C/TT-520 S-Band Transponder (x2)	5	10	1	100	10	100	10	100	10	100	10
Downlink	CAVU X-Transmitter	28	10	1.5	5	0.75	100	15	100	15	100	15
Manipulators	GITAI Inch Worm Robot (x4)	28	0	0	0	0	0	0	0	0	20	160
Storage	Custom	28	0	0	0	0	0	0	0	0	100	5
LiDAR	RVS 3000-X	28	0	0	0	0	100	97	73	70.81	73	70.81
Wide Camera	Quadclops	28	60	15	60	15	100	25	100	25	100	25
OBC(A)	Constellation	28	100	26	100	26	100	26	100	26	100	26
AI Computer	DGX Spark	28	100	75	100	75	100	75	100	75	100	75

D. Risk

Table 16 Project OSCAR Risk Table. The risks identified for Project OSCAR are organized by their risk ID, a title for the risk, a brief description of the risk, and the strategy used to mitigate said risk. The likelihood and severity of the risk are shown before and after mitigation is shown in Figure 12.

Risk ID	Risk Title	Risk Statement	Mitigation Strategy
Mission and Payload Risks			
M.1	Thruster Failure During Inspection	If the thrusters fail when inspecting the client satellite, then OSCAR will crash into the client.	Perform an Rbar approach instead of a Vbar approach so that OSCAR is never in the trajectory of the satellite.
M.2	ADACS Sensor Failure	If an ADACS Sensor fails, then OSCAR will not know its position or be able to complete the mission.	A GPS system is added to OSCAR as a secondary position tracking sensor. Additionally, there are 4 different types of sensors on the satellite for redundancy.
M.3	Missed Maneuver Window (J2 RAAN)	If OSCAR misses the maneuver window for J2 RAAN precession, then the mission can fail or spend excessive Δv.	A buffer is given in the wait period to make sure to make RAAN changes.
M.4	Probe Spreader Cold-Weld Risk	If the probe's level spreaders grip the walls of the AKM's chamber and prevent the probe from exiting the nozzle, then it may cold-weld the walls of the chamber.	Adapt level spreader curvature to reduce contact pressure, coat spreaders, use material unlikely to cold-weld.

Risk ID	Risk Title	Risk Statement	Mitigation Strategy
M.5	Propulsion/Payload Integration Failure	If the Propulsion and Payload Units are unable to unify, then the spacecraft will be unable to maneuver its payload and complete the mission.	Fine tuning approach and capture speed to minimize risk of failure and minimize physical damage from accidental impact by staying well below the aluminum frame's yield strength.
M.6	Failure to Anchor to Client	If the spacecraft is unable to anchor to the client, then it cannot provide any replacement services.	Fine tuning approach and capture speed to minimize risk of failure and minimize physical damage from accidental impact by staying well below the aluminum frame's yield strength.
M.7	Robotic Arm Collision	If the robotic arm collides with the client, it may damage itself or the client.	Robotic arms have integrated camera systems.
M.8	Replacement Component Degradation	If the replacement batteries (or other replacement components) degrade en route to the client, there will be no components to replace, resulting in a mission failure.	Replacement components will have a thermally insulated storage system.
M.9	Star Tracker Failure (Van Allen Belts)	If the satellite travels in or close to the Van Allen belts, the star tracker will fail in such conditions.	Sun sensors, magnetometers, and gyroscopes are included on the satellite for additional position determination and redundancy.
M.10	Insufficient Catalyst Preheat	If the catalyst preheat is insufficient, the green monopropellant may not ignite and will perform poorly.	Add thermal margin, closed-loop heater control, pre-burn warmup timelines, and ground test validation of cold-start and hot-start cases.
M.11	Plume Contamination	If AF-M315E plume or decomposition products land on the client's surface, then contamination may damage sensitive components.	Enforce keep-out zones, cant thrusters away from the client, and validate plume geometry in analysis.
M.12	Uneven Propellant Depletion	If there is uneven depletion or tank geometry effects, then the spacecraft's balance, attitude control, and precision burns will be difficult to operate.	Use diaphragm/bladder/managed tank design where appropriate, model depletion cases, and include control authority margin in ADACS design.

Acknowledgments

The authors gratefully acknowledge and thank Dr. Kevin Shinpaugh, Dr. Randy Spicer, Tejas Vinod, and Mathis Shinnick for their guidance and support during the design of Project OSCAR. Their technical, systems, and business knowledge improved Project OSCAR's overall design and purpose. The authors also thank the organizers, judges, and supporters of the COSMIC Capstone Challenge for their guidance and opportunity to present Project OSCAR's conceptual mission. Finally, the authors thank the Kevin T. Crofton Department of Aerospace and Ocean Engineering at Virginia Tech for the opportunity to join the COSMIC Capstone Challenge and travel to present at NASA Goddard Space Flight Center.

References

[1] Cosmic Capstone Challenge Organizers, "Cosmic Capstone Challenge (C3) Track 3 Information Package," https://cosmicspace.org/wp-content/uploads/2025/10/C3-2025-26-Information-Packet-Fall-Update.pdf, 2024. Accessed: 2026-04-08.

[2] SpaceX, *SpaceX Rideshare User's Guide*, SpaceX, 2023. URL https://www.spacex.com/rideshare/, accessed: 2026-04-07.

[3] Space Exploration Technologies Corp. (SpaceX), "SpaceX Rideshare Mission Search Results," , 2026. URL https://rideshare.spacex.com, accessed: 2026-04-07.

[4] National Aeronautics and Space Administration, "Project Gemini Familiarization Manual: Volume II — Rendezvous and Docking Configurations," Tech. Rep. SEDR 300, NASA, 1964. Copy No. unknown; Project Gemini program documentation.

[5] MakeItFrom.com, "MakeItFrom.com: Material Properties Database," , 2009. URL https://www.makeitfrom.com/.

[6] Mingtai Aluminum, "7075 vs 6061 Machinability," , 2025. URL https://www.mingtai-aluminium.com/7075-vs-6061-machinability.html, accessed: 2026-04-10.

[7] ASM International, *ASM Handbook, Volume 16: Machining*, ASM International, 2010.

[8] Ansys, "Systems Tool Kit (STK), Version 13," https://www.ansys.com/products/missions/ansys-stk, 2024. Accessed: 2026-04-10.

[9] Busek Co. Inc., *BHT-1500 Hall Effect Thruster*, Busek Co. Inc., Aug. 2021. URL https://static1.squarespace.com/static/60df2bfb6db9752ed1d79d44/t/61292a6a6a852874bb123c23/1630087786826/BHT_1500_v1.0.pdf, version 1.0, product datasheet.

[10] Spores, R. A., Masse, R., Kimbrel, S., and McLean, C., "GPIM AF-M315E Propulsion System," *50th AIAA/ASME/SAE/ASEE Joint Propulsion Conference & Exhibit*, American Institute of Aeronautics and Astronautics, 2014. URL https://ntrs.nasa.gov/api/citations/20140012587/downloads/20140012587.pdf.

[11] Gilligan, R., and Tomsik, T., "Modeling ARRM Xenon Tank Pressurization using 1D Thermodynamic and Heat Transfer Equations," Thermal & Fluids Analysis Workshop (TFAWS 2016), NASA Ames Research Center, Mountain View, CA, Aug. 2016. URL https://ntrs.nasa.gov/api/citations/20170003928/downloads/20170003928.pdf, conference presentation.

[12] "US Patent 8,016,242," , Sep. 2011. URL https://patents.google.com/patent/US8016242B2.

[13] GITAI, "GITAI Inchworm Robot for In-Space Servicing, Assembly, and Manufacturing," https://gitai.tech/inchworm-robot/, ???? Accessed: 2026-04-06.

[14] GITAI USA, Inc., "Inchworm Robot (IN Series) Brochure," https://gitai.tech/wp-content/uploads/2023/04/Inchworm-Brochure-Web.pdf, 2023. Accessed: 2026-04-06.

[15] NASA, "Gecko Grippers: Moving On Up," , 2024. URL https://www.nasa.gov/missions/station/gecko-grippers-moving-on-up/.

[16] Atkinson, M., Gliniak, C., Hull, S., Hyde, T., Liou, J.-C., Nguyen, Q.-V., Walling, B., and Young, E., "NOAA-17 Break-up Engineering Investigation Board Final Report," Tech. rep., NASA, 2021. URL https://ntrs.nasa.gov/api/citations/20240000154/downloads/20200717_Formal_Report_Template-NOAA-17-Combined.pdf.

[17] Beyond Gravity, "Constellation On Board Computer," , 2025. URL https://www.beyondgravity.com/en/satellites/electronic-solutions/computer-and-data-handling.

[18] Airbus Defense and Space, "Pureline Amethyst," , 2022. URL https://www.airbus.com/sites/g/files/jlcbta136/files/2024-12/Datasheet_SpE_PureLine_Amethyst_2022.pdf.

[19] Beyond Gravity, "Remote Terminal Unit (RTU)," , 2025. URL https://www.beyondgravity.com/en/satellites/electronic-solutions/computer-and-data-handling.

[20] NASA, "Landsat 8 Mission," , 2024. URL https://science.nasa.gov/mission/landsat-8/.

[21] NASA, "Landsat 9 Mission," , 2024. URL https://science.nasa.gov/mission/landsat-9/.

[22] World Meteorological Organization, "NOAA-18 Satellite Overview," , 2024. URL https://space.oscar.wmo.int/satellites/view/noaa_18.

[23] L3Harris Technologies, "C/TT-520 S-Band Multimode Transponder Datasheet," , 2020. URL https://www.l3harris.com/sites/default/files/2020-07/ims_eo_datasheet_S-Band_Transponder.pdf.

[24] NASA, "NASA Technical Report (19760014160)," Tech. rep., 1976. URL https://ntrs.nasa.gov/api/citations/19760014160/downloads/19760014160.pdf.

[25] NASA, "NASA Technical Report (20030061154)," Tech. rep., 2003. URL https://ntrs.nasa.gov/api/citations/20030061154/downloads/20030061154.pdf.

[26] Wertz, J. R., and Larson, W. J., *Space Mission Analysis and Design*, 3rd ed., Microcosm Press, 1999.

[27] CAVU Aerospace UK, "X-Band Transmitter," , 2023.

[28] Printech Circuit Laboratories Ltd, "X-Band 4x4 Patch Antenna Array Datasheet," , 2023.

[29] NASA Small Satellite Institute, "State of the Art: Communications," , 2023. URL https://www.nasa.gov/smallsat-institute/sst-soa/soa-communications/.

[30] Septentrio, "PolaRx5 GNSS Receiver Datasheet," , 2023.

[31] NASA, "Near Space Network (NSN)," , 2023. URL https://tempo.gsfc.nasa.gov/projects/NSN/.

[32] Jena-Optronik, "Data Sheet: RVS 3000 Product Family," , 2026. Product datasheet (PDF).

[33] TRL11, "Quadclops 3-4 Camera GEO Rated RPOD System," https://satsearch.co/products/trl11-quadclops, 2025. Accessed: 2026-04-10.

[34] EaglePicher Technologies, *EAP-12325 Thermal Battery*, EaglePicher Technologies, 2020. URL https://www.eaglepicher.com/sites/default/files/EAP%2012325.pdf, product datasheet.

[35] GS Yuasa, *MA190 Modular Lithium Ion Battery for Satellites*, GS Yuasa, ???? URL https://gsyuasa-lp.com/SpecSheets/MA190.pdf, product datasheet.

[36] Spectrolab, Inc., *XTE-SF (Standard Fluence): Space Qualified Triple Junction Solar Cell*, Spectrolab, Inc., ???? URL https://www.spectrolab.com/photovoltaics/XTE-SF_Data_Sheet.pdf, product datasheet.

[37] USAF Space and Missile Systems Center, "SMC-S-016 (2014) Test Requirements for Launch, Upper-Stage and Space Vehicles," , 2014. URL https://ntrl.ntis.gov/NTRL/dashboard/searchResults/titleDetail/ADA619375.xhtml.

[38] Aerojet Rocketdyne, "MR-103G 1N (0.2-lbf) Rocket Engine Assembly," , 2021. URL https://satsearch.co/products/aerojet-rocketdyne-mr-103g.

[39] Jena-Optronik, "RVS© 3000 Product Family," , 2024.

[40] AMD, "AMD Versal™ XQR Adaptive SoCs," , 2026. URL https://www.amd.com/en/products/adaptive-socs-and-fpgas/versal/space-grade.html.

[41] National Aeronautics and Space Administration (NASA), "Project Cost Estimating Capability (PCEC)," https://www.nasa.gov/ocfo/ppc-corner/pcec-project-cost-estimating-capability/, 2025. Accessed: 2026-04-09.

[42] National Aeronautics and Space Administration, "NASA Risk Management Procedural Requirements," Tech. Rep. NPR 8000.4, NASA, 2022. URL https://nodis3.gsfc.nasa.gov/displayDir.cfm?t=NPR&c=8000&s=4, accessed: 2026-04-10.